

Quantum Information Processing with Trapped Ions

M. D. Barrett^{*,†}, T. Schaetz^{**,‡}, J. Chiaverini^{*}, D. Leibfried^{*}, J. Britton^{*}, W. M. Itano^{*}, J. D. Jost^{*}, E. Knill[‡], C. Langer^{*}, R. Ozeri^{*} and D. J. Wineland^{*}

^{*}*Time and Frequency Division, NIST, Boulder, CO*

[†]*University of Otago, New Zealand*

^{**}*Max Planck Institut für Quantenoptik, Garching, Germany*

[‡]*Mathematical and Computational Sciences Division, NIST, Boulder, CO*

Abstract. We summarize two experiments on the creation and manipulation of multi-particle entangled states of trapped atomic ions - quantum dense coding and quantum teleportation. The techniques used in these experiments constitute an important step toward performing large-scale quantum information processing. The techniques also have application in other areas of physics, providing improvement in quantum-limited measurement and fundamental tests of quantum mechanical principles, for example.

Keywords: trapped ions, entanglement, information

PACS: 03.67.Lx, 32.80.Qk

INTRODUCTION

Efforts to experimentally realize the elements of quantum information processing (QIP) in the ion-trap system have been largely motivated by the proposal of Cirac and Zoller [1]. Although a long-term objective of this research is the implementation of large-scale QIP, the techniques used have more immediate and general application. For example, the tools required for QIP have been used to investigate issues of decoherence in quantum systems [2] and to test the fundamental principles of quantum mechanics [3, 4, 5]. Experiments have also demonstrated potential improvements in frequency metrology [6].

The ion-trap scheme satisfies the main requirements for QIP as outlined by DiVincenzo [7]: (1) a scalable system of well-defined qubits, (2) a method to reliably initialize the quantum system, (3) long coherence times, (4) the existence of universal gates, and (5) an efficient measurement scheme. Most of these requirements have been demonstrated experimentally, and emphasis has now shifted towards issues of scalability and the demonstration of fundamental QIP protocols. Here, we focus on experiments carried out at NIST but note that similar work is being pursued at Aarhus, Almaden (IBM), Hamburg, Hamilton (Ontario, McMaster Univ.), Innsbruck, Los Alamos (LANL), University of Michigan, Garching (MPI), Oxford, and Teddington (National Physical Laboratory, U.K.). We begin with a brief account of the essential elements for trapped-ion QIP. This discussion is followed by an summary of two recent experiments carried out at NIST.

COHERENT QUBIT MANIPULATION

The key to the implementation of quantum gates between ions is the ability to couple the internal qubit states with their external modes of motion. In the ${}^9\text{Be}^+$ experiments at NIST, two laser beams are used to drive two-photon stimulated-Raman transitions between the two ground-state hyperfine levels $|\downarrow\rangle \equiv |F=2, m_F=-2\rangle$ and $|\uparrow\rangle \equiv |F=1, m_F=-1\rangle$, which are separated in energy by the hyperfine splitting $\omega_0/2\pi \simeq 1.25$ GHz. A detailed account of the resulting interactions can be found in [8], [9] and [10]. Here we summarize the salient features.

Since the Raman laser beams have a large detuning from any allowed transition, any excited states can be adiabatically eliminated in a theoretical description of transitions, and the interaction is that of a two-level system with an effective field, $E_{eff} = E_0 \cos(k\hat{z} - \omega t + \phi)$. Here ω and ϕ are, respectively, the relative frequency and phase of the two Raman beams, and k is the component of the difference k-vectors for the two Raman beams associated with the motion for the selected mode. We take $\hat{z} = z_0(a + a^\dagger)$, where a and a^\dagger are the lowering and raising operators for the harmonic oscillator of the selected motional mode (frequency ω_z), and $z_0 \equiv \sqrt{\hbar/2m\omega_z}$ is the spread of the ground-state wavefunction. When the relative detuning of the Raman beams is close to ω_0 the effective Hamiltonian describing the coupling between the motional and internal states of the qubit is given, in the interaction picture, by ($\hbar = 1$)

$$H_I = \Omega \sigma^+ e^{-i((\omega - \omega_0)t + \phi)} D(i\eta e^{i\omega_z t}) + h.c., \quad (1)$$

where we have made use of the rotating-wave approximation [8]. Here, Ω is the two-photon Rabi rate, $\sigma^+ = |\uparrow\rangle\langle\downarrow|$, $\eta \equiv kz_0$ is the Lamb-Dicke parameter, and $D(\alpha) = \exp(\alpha a^\dagger - \alpha^* a)$ is the displacement operator. In the Lamb-Dicke limit ($\eta \ll 1$) the Hamiltonian can be further simplified by expanding the displacement operator to first order in η . Although we have neglected terms associated with AC stark shifts from the Raman beams, their polarizations can be chosen so as to eliminate these effects [9].

For certain choices of ω , H_I is resonant and the spin can be efficiently coupled to the motion. For example, when $\omega = \omega_0 - \omega_z$ the Hamiltonian gives rise to transitions $|\downarrow; n\rangle \leftrightarrow |\uparrow; n-1\rangle$. These are usually called "red-sideband" transitions and are an essential part of sideband laser cooling [11]. When $\omega = \omega_0$, $H_I \simeq \Omega \sigma^+ e^{i\phi} + h.c.$ and transitions no longer involve the motion ($|\downarrow; n\rangle \leftrightarrow |\uparrow; n\rangle$). These "carrier" transitions are used to perform single-qubit rotations

$$R(\theta, \phi) = \cos(\theta/2)I + i \sin(\theta/2) \cos(\phi) \sigma_x + i \sin(\theta/2) \sin(\phi) \sigma_y, \quad (2)$$

where I is the identity operator, σ_x , σ_y , and σ_z denote the Pauli spin matrices in the $\{|\uparrow\rangle, |\downarrow\rangle\}$ basis ($|\uparrow\rangle \equiv (1, 0)$, $|\downarrow\rangle \equiv (0, 1)$), θ is proportional to the duration of the Raman pulse, and ϕ is the relative phase of the Raman beams as indicated above.

We note that, for each ion, we are free to choose $\phi = 0$ for the first pulse by using the unitary transformation $|\uparrow\rangle \rightarrow e^{i\phi} |\uparrow\rangle$, $|\downarrow\rangle \rightarrow |\downarrow\rangle$. However, all subsequent operations must be referenced to this choice. For example, consider a simple two-ion experiment in which we apply two pulses corresponding to $R(\pi/4, 0)$. Before applying the second pulse we alter the trapping potential so that the second ion moves an

amount δz such that $k\delta z = \pi$. For the first ion, the net operation is given simply by $R(\pi/4, 0)R(\pi/4, 0) = R(\pi/2, 0)$. However, for the second ion, the additional phase shift due to the ion movement results in $R(\pi/4, \pi)R(\pi/4, 0) = I$. Thus, the net effect is a $\pi/2$ -pulse on the first ion only. In this way we can implement individual qubit rotations without the need for individual laser beam addressing [3, 12, 13, 14].

At the beginning of a typical experiment, laser cooling initializes the qubits to the ground states of their relevant collective motional modes [11], and they are each optically pumped to their internal state $|\downarrow\rangle$. Detection of the internal state is achieved through state-dependent resonance fluorescence measurements [3], which efficiently distinguish $|\downarrow\rangle$ (bright) from $|\uparrow\rangle$ (dark).

ENTANGLEMENT

A fundamental requirement for quantum computing is an entangling operation. A number of such operations have been investigated in the ion-trap system. The CNOT gate as proposed by Cirac and Zoller [1] has been demonstrated by the Innsbruck group [15]. A CNOT and π -phase gate, between the motion and spin qubit for a single ion, have been realized at NIST [8, 16, 17]. Also, using the scheme suggested by Sørensen and Mølmer [18, 19] and Solano *et al.* [20], a gate between two spin qubits was realized [12, 21]. A gate that has proven very robust and experimentally flexible in a number of recent experiments [6, 13, 14] is the phase gate reported in [10].

When the Raman beams, as discussed above, have a relative detuning close to a mode frequency ($\omega_z + \delta$), the effective Hamiltonian for a single ion in the interaction picture is given by

$$H_I = \sum_{m_S=\uparrow, \downarrow} \eta \Omega_{m_S} (e^{i(\delta t + \phi)} a + e^{-i(\delta t + \phi)} a^\dagger) |m_S\rangle \langle m_S|. \quad (3)$$

Here we have taken the Lamb-Dicke limit and kept only the near-resonant terms. As before we have neglected Stark shifts as they can be eliminated with an appropriate choice of polarizations. Also, for our particular implementation, we have $\Omega_\downarrow = -2\Omega_\uparrow$ [9, 10]. As discussed in [9, 10], this Hamiltonian describes the off-resonant sinusoidal forcing of the ion with a spin-dependent force amplitude and originates from the dipole force induced by the Raman beams. We note that the phase ϕ can no longer be transformed away and depends on the ion's position. In the two-ion phase gate discussed in [10] the ions are separated by a distance such that the Raman beam phase difference between the two ions is a multiple of 2π . In this case the Hamiltonian for the two ion system takes the simple form

$$H_I = \Omega_D (e^{i(\delta t + \phi)} a + e^{-i(\delta t + \phi)} a^\dagger) (|\uparrow\downarrow\rangle \langle\uparrow\downarrow| - |\downarrow\uparrow\rangle \langle\downarrow\uparrow|), \quad (4)$$

where Ω_D is the total driving force on the two ions. This Hamiltonian can be easily integrated and after a time $2\pi/\delta$ yields the transformation

$$|\uparrow\uparrow\rangle \rightarrow |\uparrow\uparrow\rangle, |\uparrow\downarrow\rangle \rightarrow e^{i\Phi} |\uparrow\downarrow\rangle, |\downarrow\uparrow\rangle \rightarrow e^{i\Phi} |\downarrow\uparrow\rangle, |\downarrow\downarrow\rangle \rightarrow |\downarrow\downarrow\rangle,$$

where $\Phi = -|\Omega_D|^2 t / \delta$. Experimentally we set δ and t so that $\Phi = -\pi/2$.

Although we have restricted our discussion to two ions we note that the phase gate can be applied in more general situations. Indeed it has been successfully applied in three ion experiments [6, 13] and can potentially be applied when a different species is present, as in sympathetic cooling experiments [22]. Additionally, the phase gate is robust against small amounts of heating (provided the Lamb-Dicke limit is satisfied). Indeed, even when one of the motional modes has a thermal energy as large as $\bar{n} = 1$, the gate still has a fidelity as high as 0.9 [13]. Also the phase gate does not require individual addressing, is carried out by a single pulse, and does not require the use of an additional internal state. These features have made the phase gate the entangling operator of choice for our recent experiments.

QUANTUM DENSE CODING

Quantum dense coding [23] enables the communication of two bits of classical information with the transmission of a single qubit. Two parties, Alice and Bob, each hold one qubit of a maximally entangled pair that has been previously prepared and distributed. With this as a starting point, Bob applies one of four possible unitary operations (each identified with the states of two classical bits) to his qubit and then transmits it to Alice. Once received, Alice performs a Bell-state measurement on the two qubits. From the outcome of this measurement Alice can deduce unambiguously which of the four operations Bob used and the corresponding classical bits of information.

Our implementation of the dense-coding protocol is illustrated in Fig. 1, and a detailed account is given in [14]. First, the ions are cooled to the ground state of both axial modes of motion and optically pumped to $|\downarrow\downarrow\rangle$. The ions are then prepared in a maximally entangled state by applying a $\pi/2$ -pulse ($R(\pi/2, -\pi/2)$), followed by the phase gate as outlined above. This leaves the ions in the state $|\Phi_+\rangle = |-Y\rangle_B |\downarrow\rangle_A + |Y\rangle_B |\uparrow\rangle_A$, where $|+Y\rangle = |\uparrow\rangle + i|\downarrow\rangle$ and $|-Y\rangle = i|\uparrow\rangle + |\downarrow\rangle$ are the eigenstates of σ_y ($\sigma_y|\pm Y\rangle = \pm|\pm Y\rangle$). (For convenience of notation, we omit normalization factors.) Next, one of the four operations I , σ_x , σ_y , or σ_z is applied to ion B by use of the individual addressing technique discussed earlier (encoding step). This operation takes initial state, $|\Phi_+\rangle$, to one of the four Bell states $\{|\Phi_\pm\rangle, |\Psi_\pm\rangle\}$ where $|\Phi_\pm\rangle = |-Y\rangle_B |\downarrow\rangle_A \pm |Y\rangle_B |\uparrow\rangle_A$, and $|\Psi_\pm\rangle = |Y\rangle_B |\downarrow\rangle_A \pm |-Y\rangle_B |\uparrow\rangle_A$. Finally, a Bell-state measurement is performed by applying the phase-gate and a $\pi/2$ -pulse ($R(\pi/2, -\pi/2)$) before individually detecting each ion. We note that the final phase-gate and $\pi/2$ -pulse effects a basis transformation (decoding step) from the Bell-state basis $\{|\Phi_\pm\rangle, |\Psi_\pm\rangle\}$ to the measurement basis $\{|\uparrow\uparrow\rangle, |\downarrow\downarrow\rangle, |\uparrow\downarrow\rangle, |\downarrow\uparrow\rangle\}$. Ideally the four measurement outcomes, $|\uparrow\uparrow\rangle, |\downarrow\downarrow\rangle, |\uparrow\downarrow\rangle$, and $|\downarrow\uparrow\rangle$ can be unambiguously associated with the operators $\sigma_x, \sigma_y, \sigma_z$, and I respectively. Experimentally, imperfections result predominately from the two phase-gate operations and the individual addressing operation. The average fidelity associated with all four operations is 0.85(1). We also estimate a channel capacity of 1.16(1), which exceeds the maximum classical result of 1.

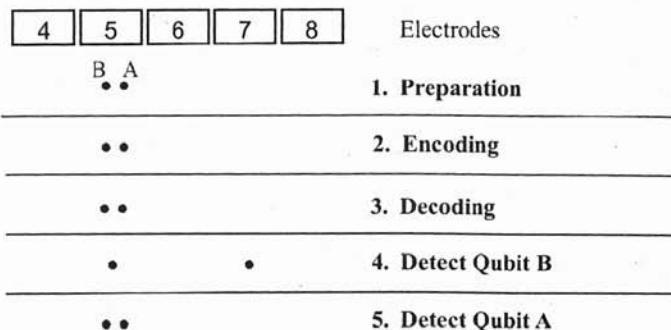


FIGURE 1. Schematic diagram of the dense-coding implementation using atomic qubits. In the top part of the figure, relevant trapping zones used in the experiment (not to scale) are numbered. To facilitate individual detection of the qubits, qubit B (left) is measured and then transferred to a non-fluorescing state, followed by detection of qubit A (right).

QUANTUM TELEPORTATION

Quantum teleportation [24] provides a means to transport quantum information efficiently from one location to another, without the physical transfer of the associated quantum-information carrier. This is achieved by using the non-local correlations of previously distributed, entangled qubits. Teleportation is expected to play an integral role in quantum communication [25] and quantum computation [26]. Implementation of quantum teleportation is therefore an important benchmark for comparison of QIP in other physical systems. Our demonstration [13] is also important as it incorporates most of the techniques necessary for scalable QIP in an ion-trap system [8, 27].

Previous experimental demonstrations have been implemented with optical systems that used both discrete and continuous variables [28], and with liquid-state nuclear magnetic resonance [29]. Our demonstration [13] and that of the Innsbruck group [30] are the first demonstrations of teleportation using atomic qubits. Aside from obvious differences in the experimental implementations the basic protocol is the same [24]. Alice is in possession of a qubit (here labelled 2) that is in an unknown state $|\psi\rangle_2 \equiv \alpha|\uparrow\rangle_2 + \beta|\downarrow\rangle_2$. In addition, Alice and Bob each possess one qubit of a two-qubit entangled pair that we take to be a singlet $|S\rangle_{1,3} \equiv |\uparrow\rangle_1|\downarrow\rangle_3 - |\downarrow\rangle_1|\uparrow\rangle_3$. Therefore, Alice possesses qubits 1 and 2, while Bob holds qubit 3. The initial joint state of all three qubits is

$$|\Phi\rangle = |S\rangle_{1,3} \otimes |\psi\rangle_2. \quad (5)$$

This state can be rewritten using an orthonormal basis of Bell states $|\Psi_k\rangle_{1,2}$ ($k=1,2,3,4$) for the first two qubits and unitary transformations $\{U_k\}$ acting on $|\psi\rangle_3$ ($= \alpha|\uparrow\rangle_3 + \beta|\downarrow\rangle_3$) so that $|\Phi\rangle = \sum_{k=1}^4 |\Psi_k\rangle_{1,2} (U_k|\psi\rangle_3)$. A measurement in the Bell-state basis $\{|\Psi_k\rangle_{1,2}\}$ by Alice then leaves Bob with one of the four possibilities $U_k|\psi\rangle_3$. Once Bob learns of Alice's measurement outcome (through classical communication), he can recover the original unknown state by applying the appropriate unitary operator U_k^{-1} to his state $U_k|\psi\rangle_3$. We note that Alice's Bell-state measurement can be accomplished by

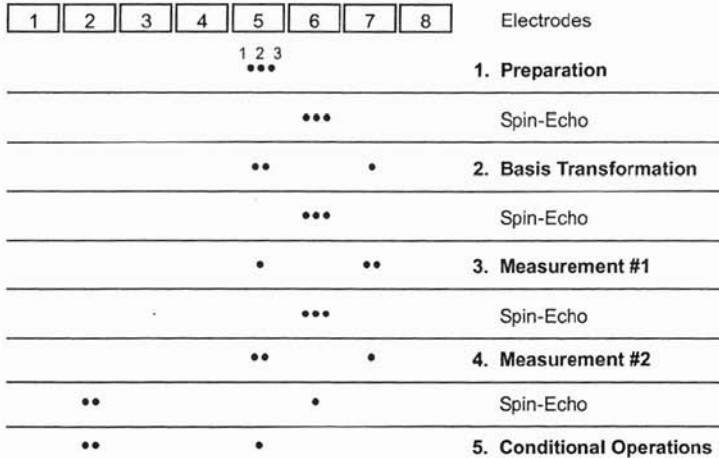


FIGURE 2. Schematic diagram of the teleportation implementation using atomic qubits. Ions are numbered left to right as indicated at the top. In step 1, we prepare the outer ions in the singlet state and the middle ion in an arbitrary state. Steps 2-4 constitute a Bell-state measurement on ions 1 and 2, teleporting the state of ion 2 onto ion 3, up to unitary operations that depend on the measurement outcomes. In step 5 the conditional operations are applied, recovering the initial state. Interspersed are spin-echo pulses that protect the state from dephasing due to fluctuating magnetic fields but do not affect the teleportation protocol.

transforming from the basis $\{|\Psi_k\rangle_{1,2}\}$ into the measurement basis $\{|\uparrow\uparrow\rangle, |\downarrow\uparrow\rangle, |\uparrow\downarrow\rangle, |\downarrow\downarrow\rangle\}$ as in the dense-coding experiment.

Our implementation of the quantum teleportation protocol is illustrated in Fig. 2 and a more detailed account can be found in [13]. Briefly, we first prepare the ions in the state $|S\rangle_{1,3} \otimes |\downarrow\rangle_2$ in two steps. First a phase gate is combined with individual rotations to produce the state $(|\downarrow\downarrow\rangle_{1,3} - i|\uparrow\uparrow\rangle_{1,3}) \otimes |\downarrow\rangle_2$. Then an individual addressing operation is used to produce $|S\rangle_{1,3}$ from the state $|\downarrow\downarrow\rangle_{1,3} - i|\uparrow\uparrow\rangle_{1,3}$. For the state $|S\rangle_{1,3} \otimes |\downarrow\rangle_2$, ions 1 and 3 are in the singlet state, which is invariant to a global rotation. Therefore an arbitrary global rotation $R(\theta, \phi)_{1,2,3}$ applied to all three ions rotates the middle ion without affecting the outer two. In this way we can prepare the state $|\Phi\rangle$ of Eq. 5 for any α and β . To teleport the state of ion 2 to ion 3 we first implement a Bell-state measurement on ions 1 and 2. This is achieved by applying the phase gate and a $\pi/2$ -pulse ($R(\pi/2, 0)$) to ions 1 and 2 before individual detection. As in the quantum dense-coding protocol, the phase gate and $\pi/2$ -pulse effect a basis transformation from the Bell-state basis to the measurement basis. The teleportation is then completed by applying unitary operations on ion 3, conditioned on the measurement outcomes on ions 1 and 2. In our implementation these unitary operators are simply a $\pi/2$ -pulse ($R(\pi/2, \pi/2)$) followed by the operators $\sigma_x, \sigma_y, I, \sigma_z$ for the measurement outcomes $|\uparrow\uparrow\rangle_{1,2}, |\uparrow\downarrow\rangle_{1,2}, |\downarrow\uparrow\rangle_{1,2}, |\downarrow\downarrow\rangle_{1,2}$ respectively. In the experiment additional spin-echo pulses $R(\pi, \phi_{SE})$ are used to prevent dephasing due to variations in the ambient magnetic field on a time scale longer than the duration between pulses [10, 13]. Inclusion of these pulses does not fundamentally change the teleportation protocol; however, for

$\phi_{SE} = \pi/2$, we must reorder the operations following the $\pi/2$ -pulse, $R(\pi/2, \pi/2)$, to $I, \sigma_z, \sigma_x, \sigma_y$ respectively.

By teleporting a range of states ($|\uparrow\rangle, |\downarrow\rangle, |\uparrow\rangle \pm |\downarrow\rangle, |\uparrow\rangle \pm i|\downarrow\rangle$) we can infer an average fidelity over the entire Bloch sphere of 0.78(2). This exceeds the upper bound of $2/3$ for any classical protocol, which doesn't use entanglement[31]. Although teleportation has been demonstrated in other systems, our demonstration incorporates teleportation into a simple experiment in such a way that it can be viewed as a subroutine of a quantum algorithm; a Ramsey experiment on two spatially-separated qubits. Furthermore, our demonstration incorporates most of the important features required for large-scale quantum information processing using trapped ions [8, 27]: We (a) reliably select qubits from a group and move them to separate trap zones while maintaining their entanglement, (b) manipulate and detect qubits without the need for strongly focused laser beams, and (c) perform quantum logic operations conditioned on ancilla measurement outcomes.

CONCLUSIONS AND FUTURE OUTLOOK

The experiments discussed here demonstrate the use of entanglement as a resource in a manner that is scalable to many qubits. The two protocols are somewhat complementary: dense-coding communicates two bits of classical information by transmitting one qubit, whereas teleportation communicates one qubit of information by transmitting two classical bits. The success of the latter may seem a bit surprising since, in general, it takes an infinite amount of classical information to characterize a qubit superposition state. Yet, with the added resource of prior shared qubits from an entangled pair (with their intrinsic quantum correlations), only two classical bits are required to transmit the qubit state.

Although large-scale quantum information processing is still in the distant future, experiments such as the ones described here are key ingredients to achieving scalability. If the fidelity of these protocols can be improved sufficiently, large-scale quantum computation is, in principle, possible [32]. Therefore, future work will be devoted to reduction of technical noise, which currently limits operation fidelity, and to the construction of ion-trap arrays [8, 27] that can provide the necessary scalability.

ACKNOWLEDGMENTS

We thank David Hume and Jeroen Koelemeij for comments on the manuscript. This work was supported by the U. S. National Security Agency (NSA), the Advanced Research and Development Activity (ARDA) and NIST. This manuscript is a publication of NIST and is not subject to U. S. copyright.

REFERENCES

1. J. I. Cirac and P. Zoller, Quantum computations with cold trapped ions, *Phys. Rev. Lett.* **74**, 4091 (1995).

2. C. J. Myatt, *et al.*, Decoherence of quantum superpositions through the coupling to engineered reservoirs. *Nature* **403**, 269-273 (2000).
3. M.A. Rowe, *et al.*, Experimental violation of a Bell's inequality with efficient detection, *Nature*, **409**, 791 (2001).
4. C. F. Roos, *et al.*, Control and measurement of three-qubit entangled states, *Science*, **304**, 1478 (2004).
5. D. Moehring *et al.*, Experimental Bell inequality violation with an atom and a photon, *Phys. Rev. Lett.* **93**, 090410 (2004).
6. D. Leibfried, *et al.*, Toward Heisenberg-limited spectroscopy with multiparticle entangled states, *Science*, **304**, 1476-1478 (2004).
7. D. P. DiVincenzo, in *Scalable Quantum Computers*, edited by S. L. Braunstein and H. K. Lo (Wiley-VCH, Berlin, 2001), pp. 1-3.
8. D. J. Wineland, *et al.*, Experimental issues in coherent quantum-state manipulation of trapped atomic ions, *J. Res. Nat. Inst. Stand. Tech.* **103**, 259 (1998).
9. D. J. Wineland, *et al.*, Quantum information processing with trapped ions, *Phil. Trans. R. Soc. Lond. A* **361**, 1349-1361 (2003).
10. D. Leibfried, *et al.*, Experimental demonstration of a robust, high-fidelity geometric two ion-qubit phase gate, *Nature*, **422**, 412-415 (2003).
11. C. Monroe, *et al.*, Resolved-sideband Raman cooling of a bound atom to the 3D zero-point energy, *Phys. Rev. Lett.* **75**, 4011 (1995).
12. D. Kielpinski, *et al.*, A decoherence-free quantum memory using trapped ions, *Science* **291**, 1013 (2001).
13. M. D. Barrett, *et al.*, Deterministic quantum teleportation of atomic qubits, *Nature*, **429**, 737-739 (2004).
14. T. Schaez, *et al.*, Quantum dense-coding with atomic qubits, *Phys. Rev. Lett.* **93** 040505 (2004).
15. F. Schmidt-Kaler, *et al.*, Realization of the Cirac-Zoller controlled-NOT quantum gate. *Nature* **422**, 408-411 (2003).
16. C. Monroe *et al.*, Demonstration of a fundamental quantum logic gate. *Phys. Rev. Lett.* **75**, 4714-4717 (1995).
17. B. DeMarco, *et al.*, Experimental demonstration of a controlled-NOT wave-packet gate, *Phys. Rev. Lett.* **89**, 267901 (2003).
18. A. Sørensen and K. Mølmer, Quantum computation with ions in thermal motion. *Phys. Rev. Lett.* **82**, 1971 (1999).
19. A. Sørensen and K. Mølmer, Entanglement and quantum computation with ions in thermal motion, *Phys. Rev. A.* **62**, 02231 (2000).
20. E. Solano *et al.*, Deterministic Bell states and measurement of the motional state of two trapped ions, *Phys. Rev. A.* **59**, 2539 (1999).
21. C. A. Sackett *et al.*, Experimental entanglement of four particles, *Nature* **404**, 256 (2000).
22. M. D. Barrett *et al.*, Sympathetic cooling of $^9\text{Be}^+$ and $^{24}\text{Mg}^+$ for quantum logic, *Phys. Rev. A.* **68**, 042302 (2003).
23. C. H. Bennett and S. J. Wiesner, Communication via one- and two-particle operators on Einstein-Podolsky-Rosen states, *Phys. Rev. Lett.* **69**, 2881 (1992).
24. C. H. Bennett, *et al.*, Teleporting an unknown quantum state via dual classical and Einstein-Podolsky-Rosen channels, *Phys. Rev. Lett.* **70**, 1895-1899 (1993).
25. H.-J. Briegel, *et al.*, Quantum repeaters: The role of imperfect local operations in quantum communication, *Phys. Rev. Lett.* **81**, 5932 (1998).
26. D. Gottesman and I. L. Chuang, Demonstrating the viability of quantum computation using teleportation and single bit operations, *Nature* **402**, 390-393 (1999)
27. D. Kielpinski, C. R. Monroe, and D. J. Wineland, Architecture for a large-scale ion-trap quantum computer, *Nature* **417**, 709-711 (2002).
28. D. Bouwmeester *et al.*, Experimental quantum teleportation, *Nature* **390**, 575-579 (1997); A. Furusawa *et al.*, Unconditional quantum teleportation, *Science* **282**, 706-709 (1998); D. Boschi, *et al.*, Experimental realization of teleporting an unknown pure quantum state via dual classical and Einstein-Podolsky-Rosen channels, *Phys. Rev. Lett.* **80**, 1121-1125 (1998); Y.-H. Kim, *et al.*, Quantum teleportation of a polarization state with a complete Bell state measurement, *Phys. Rev. Lett.* **86**, 1370-1373; W. P. Bowen *et al.*, Experimental investigation of continuous-variable quantum teleportation,

- Phys. Rev. A. **67**, 032302 (2003); T. C. Zhang *et al.*, Quantum teleportation of light beams, Phys. Rev. A. **67**, 033802 (2003).
29. M. A. Nelson *et al.*, Complete quantum teleportation using nuclear magnetic resonance, Nature **396**, 52-55 (1998).
 30. M. Riebe *et al.*, Deterministic quantum teleportation with atoms, Nature **429**, 734-737 (2004).
 31. M. Massar and S. Popescu, Optimal extraction of information from finite quantum ensembles, Phys. Rev. Lett. **74**, 1259-1263 (1995).
 32. J. Preskill, Reliable Quantum Computers, Proc. R. Soc. Lond. A **454**, 385 (1998).